DOI: 10.1002/ejic.200700995

Benzylamines as Versatile Agents for the One-Pot Synthesis and Highly Ordered Stacking of Anatase Nanoplatelets

Georg Garnweitner,*[a] Ninjbadgar Tsedev,[b] Hanno Dierke,[c] and Markus Niederberger[d]

Keywords: Nanostructures / Layered compounds / Titanium / Nonaqueous synthesis / Hybrid materials

The simple reaction of titanium isopropoxide in benzylamine is shown to lead to remarkably complex, highly ordered hybrid structures. These structures consist of anatase nanoplatelets that were stacked in a lamellar fashion with a small organic layer in between. By careful characterization of these structures, we show that indeed solely the benzylamine solvent is present in the organic moiety between the nanocrystals, which thereby provides both shape control and alignment of the inorganic crystals. The solvent also plays a central role during the anatase formation itself; hence, it enacts control on the forming materials on a multitude of levels.

Introduction

Hybrid organic–inorganic materials are one of the hottest topics in research today, and one struggles to combine the advantages of organic and inorganic components of the material whilst eliminating their limitations.[1,2] Although also macroscopic composites have proven their advantageous properties to mankind,[2] the full potential of hybrid materials is unfolded in nanocomposites, where the interface of chemistry and physics come to play a dominant role.[3] These materials can exhibit a multitude of structures, ranging from inorganic clusters or nanoparticles embedded in organic polymers[4,5] to organically modified inorganic materials such as ORMOSILs (organically modified silicas).[6] Sol–gel strategies are an ideal means for the controlled synthesis of such structures, and a lot of effort has been invested in their molecular design.[7] Especially, the organic modification of metal–oxido clusters has been shown to provide high versatility for the synthesis of hybrid materials of many metal oxides.[8]

The synthetic strategies of such hybrids often involve several reaction and purification steps to achieve good control of the structure and composition of the forming material. Still, when going beyond the cluster length scale, control of size and shape, especially of the inorganic component, remains challenging. The rational design of even simple metal oxide nanoparticles, for example, is not yet possible, although complete avoidance of water in the reaction systems has led to much progress in that respect.[9,10] This nonaqueous strategy offers the great advantage that very simple reaction systems can be used, even in the absence of any surfactant, as the solvent also fulfills the role of a growth-controlling agent. This renders nonaqueous processes highly suitable for syntheses on larger scales,[11,12] but also constitutes a big advantage for performing mechanistic studies.[13] It has turned out that the role of the organic species in the system can be manifold, providing not only size and shape control but also contributing to the particle formation itself and to the stabilization of the formed nanostructures. In special systems, the organic species interact with each other, and thus help to assemble the inorganic crystals into extended hybrid composite materials. In these cases, it is even possible to create nanocomposites in a one-pot process, as we have recently shown for lamellar hybrid yttria–benzoate nanostructures.[14] Yttrium isopropoxide was treated with benzyl alcohol at elevated temperatures to result in particles consisting of alternating layers of yttria and benzoate species that were bound to the yttria surface and stacked together through π–π interactions. Pinna et al. showed that this approach is a quite general possibility for the facile synthesis of highly ordered layered nanocomposites containing lanthanide oxides.[15,16] Interestingly, in the benzyl alcohol solvent only the reaction of the rare-earth alkoxides can produce such nanocomposites, whereas the use of other transition-metal alkoxides generally results in highly crystalline nanoparticles.[17] Here, we show that by switching to benzylamines as solvents, nanocomposites can be obtained simply by the solvothermal treatment of titanium isopropoxide. The formed hybrid structures consist of elongated nanoplatelets that are arranged in a lamellar, highly ordered fashion. In order to investigate the role of the solvent in the

[a] TU Braunschweig, Institute of Particle Technology
Volkmaroder Str. 5, 38104 Braunschweig, Germany
Fax: +49-531-3919615
E-mail: G.Garnweitner@tu-bs.de
[b] Max Planck Institute of Colloids and Interfaces,
Research Campus Golm, 14424 Potsdam, Germany
[c] TU Braunschweig, Institute of Condensed Matter Physics
Mendelssohnstr. 3, 38106 Braunschweig, Germany
[d] ETH Zurich, Department of Materials
Wolfgang-Pauli-Str. 10, 8093 Zurich, Switzerland

formation of these structures, the obtained products were characterized in detail and possible formation mechanisms are given.

Results and Discussion

We have investigated the synthesis of titania nanoparticles from common titania precursors in a nonaqueous regime quite intensively by employing benzyl alcohol[18,19] and also aprotic solvents as reaction media.[20] Similar to these systems, the analogous reaction of titanium tetraisopropoxide in benzylamine, when used in a molar ratio of 1:50, yielded slightly yellow or greenish milky suspensions. After washing and drying, yellow powders were obtained that appeared rather soft and fluffy and, thus, not like a typical metal oxide powder. The samples were characterized by powder X-ray diffraction (XRD). The highest ordering was obtained when the solvothermal treatment was performed at 200 °C for 3 d. A typical diffractogram is presented in Figure 1,a. The dominant low-angle reflection at $2\theta = 7.3°$ proves the presence of a highly ordered lamellar structure, representing the 100 reflection of the lamellae. Its position corresponds to a *d* spacing of 1.2 nm. A second-order peak is visible at 14.1°. The signals at larger angles correspond to the crystal structure of the inorganic material (shown in higher magnification in Figure 1,a*). Most of the other visible peaks correspond to the anatase phase of TiO_2. The peaks, however, are rather broad, pointing towards the presence of small crystallites, except for the 200 reflection found at $2\theta = 48.3°$. This indicates that the nanocrystals possess strongly anisotropic morphology, with substantially enhanced growth in the [200] direction. Growth along the *c* axis of the anatase lattice, however, appears diminished, as the 004 reflection is strongly decreased, especially in comparison to the neighboring 112 reflection. The reflection marked *r* cannot be assigned to anatase and probably stems from a small amount of rutile present in the sample. To investigate the effects of the solvent, we performed the analogous reaction in *m*-xylylenediamine [(3-aminomethyl)benzylamine]. A similar product was obtained, the XRD plot of which is presented in Figure 1,b. Again, highly ordered structures were found, but the main small-angle reflection was slightly shifted to $2\theta = 6.3°$, corresponding to a *d* spacing of 1.4 nm. The large-angle anatase signals are quite similar to the benzylamine sample, with a slightly lower intensity of the 200 signal, which indicates a smaller size of the obtained nanocrystals along their [200] direction.

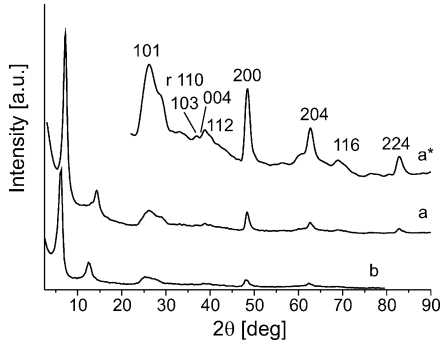

Figure 1. XRD graphs of a nanocomposite obtained from solvothermal treatment of $Ti(OiPr)_4$ in benzylamine (a) and *m*-xylylenediamine (b); wide-angle region of the benzylamine sample under higher magnification (a*).

Transmission electron microscopy (TEM) images of the sample prepared in benzylamine are presented in Figure 2 at various magnifications. The images indicate the presence of nanoplatelets that are tightly stacked, forming large aggregates several hundred nanometers in size. The stacking is highly regular, with the nanoplatelets additionally being arranged to form extensive layers in their equatorial direction. To further investigate the structure of these aggregates and to prove the platelet-like morphology of the individual nanocrystals, an image under higher magnification is shown in Figure 3,a. On the right side of the image, the nanoplatelets are visible frontally, and they are about 25–30 nm in

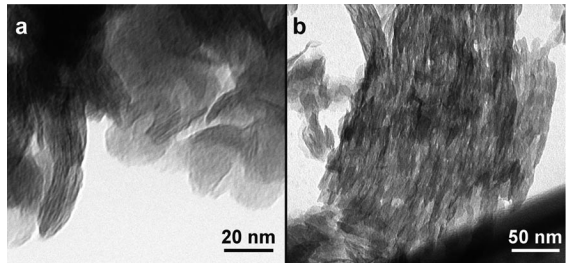

Figure 3. TEM images of the sample obtained in benzylamine at higher magnification (a) and after extensive washing and ultrasonication treatment (b).

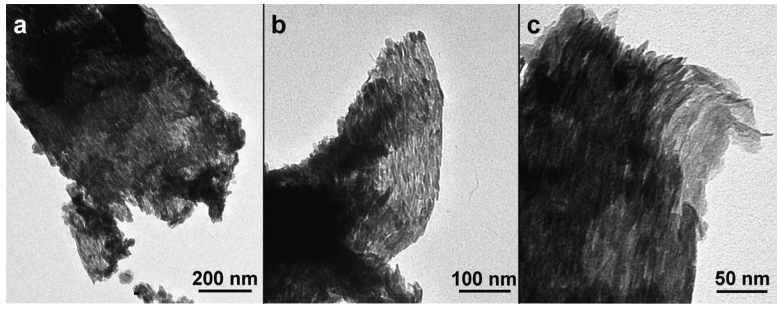

Figure 2. TEM images of the nanocomposite obtained in benzylamine under various magnifications (a, b).

size and circular to ellipsoidal in shape. In the cone-like structure on the lower left of the micrograph, however, clearly a lamellar structure is visible, consisting of dark layers alternating with light organic layers. Obviously, in this region the platelets are oriented parallel to the viewing direction. The dark layers (and, thus, the nanoplatelets) are about 0.7 nm thick and separated by organic light-contrast layers that are 0.6 nm thick, resulting in a *d* spacing of 1.3 nm, which is in good agreement to the *d* spacing of the lamellae of 1.2 nm as obtained by XRD. We thus infer that the nanoplatelets are stacked to agglomerates about 20–50 nm in thickness; however, they laterally extend over several hundred nanometers. Within the sample, these stacks are randomly oriented with respect to each other.

We propose that the formation of anatase nanoplatelets, in contrast to the bigger and spherical nanoparticles that were obtained in other solvents,[20] is a result of strong binding of the benzylamine (or *m*-xylylenediamine) solvent to the (001) surface of the nanocrystals, which thereby prevents further growth in the [001] direction. Such selectivity has been observed for anatase also with other organic species such as Trizma or oleic acid; however, it is highly interesting to note that in these cases, growth/agglomeration in the [001] direction was in fact enhanced over the other crystal faces either by surface-selective desorption (Trizma) or by surface-selective capping (oleic acid).[21,22] Examples of the influence of the crystal face-specific capping agents on the morphology of nanostructures during their liquid-phase synthesis have abounded in the last decade,[9,23] proving that in many cases selective binding of small organic molecules with specific functional groups can result in the directed growth of inorganic nanorods or nanoplatelets.[24]

As the solvent molecules preferentially bind to the (001) crystal face, the nanoplatelets are not stabilized against agglomeration on their other faces. Thus, they assemble laterally to form extensive sheet-like structures as visible in the TEM pictures. The organic layers between these stacked sheets appear quite thin, pointing towards the presence of small organic species in those layers. In contrast, the "glue" between the sheets of anatase is remarkably stable, and it was not possible to separate the anatase sheets even by applying extensive ultrasonication and washing treatments in various solvents (Figure 3,b displays a sample after extensive washing and ultrasonication in toluene, showing similar agglomerated layered structures as were observed initially).

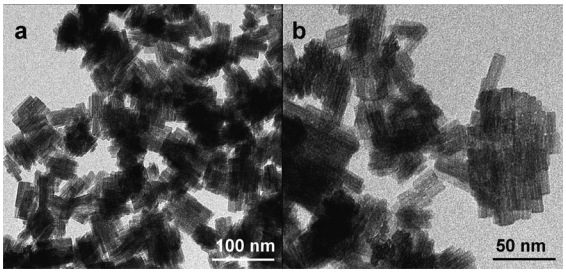

Figure 4. TEM micrographs of the sample obtained in *m*-xylylenediamine under various magnifications (a, b).

TEM images of the sample prepared in *m*-xylylenediamine are shown in Figure 4. Interestingly, the morphology is rather different in this case, as structures only about 100 nm in size are present that possess prism-like shape. It is clearly visible that these structures are also composed of stacked platelets with similar thickness to that observed in the case of benzylamine, but obviously, the assembly of the platelets in their plane direction is much less pronounced here. Assuming the presence of solvent molecules between the inorganic layers, a slightly higher organic layer thickness can be expected in this case, which is in good agreement to the larger *d* spacing observed in the XRD measurement.

Thermal analysis of the obtained nanocomposites was performed to obtain quantitative information about their composition and stability. Figure 5 presents the TGA data obtained by heating the dried products from benzylamine (a) and *m*-xylylenediamine (c) at a low heating rate of 5 °C min^{-1} up to 950 °C under an atmosphere of nitrogen. Additionally, the decomposition behavior of the benzylamine sample under an atmosphere of oxygen is shown (b). Interestingly, the sample prepared in *m*-xylylenediamine contains about 10 wt.-% more organics than the benzylamine sample. Both samples exhibit only a small weight loss of 5% up to 150 °C, pointing to a small amount of adsorbed solvents and moisture. The main decomposition step occurs between 150 and 450 °C and is attributed to the desorption and decomposition of benzylamine present on the surface of the aggregates and individual nanocrystals. This decomposition step is much more pronounced for the *m*-xylylenediamine sample, which is consistent with the presence of smaller agglomerates as observed for this sample by TEM. However, above this temperature and even at 900 °C there is a substantial further weight loss, which is attributed to the formation of amorphous carbon from the organic matter intercalated between the anatase layers of the nanostructure that decomposes only at temperatures above 800 °C. Therefore, the remarkably high temperatures required for full decomposition of the organic matter is a strong indication for the presence of thin layers of strongly bound organic matter in between the anatase platelets. Un-

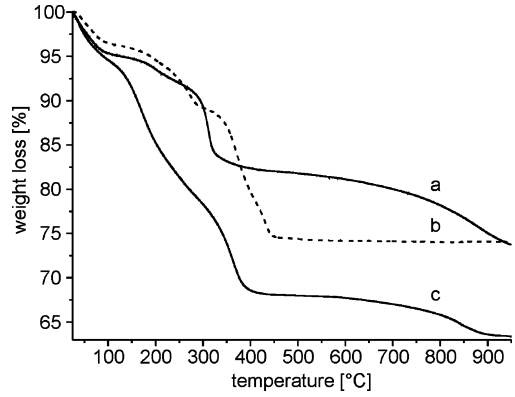

Figure 5. Thermograms of the nanocomposite prepared in benzylamine under an atmosphere of N_2 (a) and O_2 (b); thermogram of the sample obtained in *m*-xylylenediamine under an atmosphere of N_2 (c).

der an oxygen atmosphere, decomposition of the organics is enhanced due to the formation of CO_2 rather than amorphous carbon, and hence, the weight loss is completed at 500 °C. From the sample measured under an atmosphere of oxygen, the total organic content of the sample prepared in benzylamine was determined to be about 27 wt.-% and that of the *m*-xylylenediamine sample was 38 wt.-%. In contrast, anatase nanoparticles prepared by similar nonaqueous routes in other solvents that are present as individual nanoparticles show an organic content of less than 10 wt.-%, with decomposition fully completed at 500 °C also when measured under an atmosphere of nitrogen due to the much easier decomposition of the organics present on the particle surface.[20]

For further analysis of the obtained hybrid materials, diffuse reflectance infrared fourier transform spectroscopy (DRIFTS) measurements were carried out. In Figure 6, the DRIFTS spectrum of a sample obtained in benzylamine is displayed. From the intensity ratio between the inorganic Ti–O–Ti modes (ca. 550 cm^{-1}) and the organic modes (e.g., ca. 1500 cm^{-1}), it is clearly visible that the content of organics is rather high in this sample. In this spectrum, N–H stretching vibrations at 3400 cm^{-1} and the bands at 755 and 667 cm^{-1}, corresponding to the $–NH_2$ wagging vibration, clearly prove the presence of amine groups in the nanocomposite. The two latter signals are shifted relative to a free amine,[25] which indicates that there is binding of the amine group to the anatase surface. Furthermore, the signals at 1615 and 1500 cm^{-1}, attributed to C=C aromatic ring stretching, and the two peaks observed at 3064 and 3028 cm^{-1}, assigned to the asymmetric and symmetric C–H stretching modes, point towards the presence of a monosubstituted aromatic ring. Therefore, we infer that the organic layers being intercalated between the anatase platelets indeed consist of benzylamine species. The broad peak centered at 3200 cm^{-1} is caused by a hydroxy species adsorbed to the titania surface during the synthesis (see below).

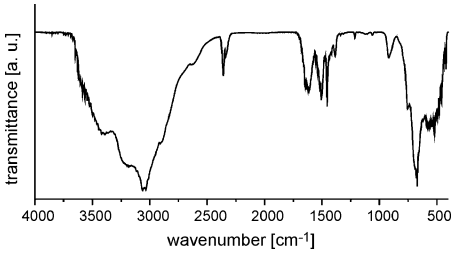

Figure 6. DRIFTS measurement of the hybrid material prepared in benzylamine.

To unambiguously prove the sole presence of benzylamine in the organic moiety between the arranged nanoplatelets, we conducted ^{13}C-MAS solid-state NMR measurements. A typical nanocomposite prepared in benzylamine was analyzed, and the corresponding spectrum obtained at a spinning rate of 7 kHz is presented in Figure 7. The peaks marked with asterisks are shifted relative to the spectrum obtained at a spinning rate of 5 kHz (not shown) and, therefore, can be identified as rotational sidebands. The remaining signals at δ = 129.0 and 43.2 ppm are somewhat broad but can be unambiguously attributed to benzylamine. The presence of any benzoic acid, benzaldehyde, or benzyl alcohol can clearly be excluded. Thus, we conclude that the benzylamine provides control over growth and assembly of the nanocrystals through selective binding of its amine groups to the (001) crystal surface. The phenyl groups of bound benzylamine next undergo π–π interactions, which therefore leads to assembly and stacking of the platelets into a highly ordered nanocomposite material.

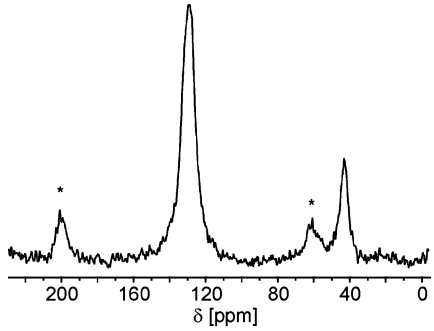

Figure 7. ^{13}C-CP MAS solid-state NMR spectrum of the nanocomposite prepared in benzylamine. The rotational sidebands are marked with asterisks.

To gain understanding of the anatase formation itself, we elucidated the formation mechanism by identifying the organic side compounds present in the final reaction solution, followed by retro analysis. The ^{13}C liquid NMR characterization of the final reaction solution (not shown) revealed that aside from the benzylamine solvent, dibenzylamine, *N*-benzylidenebenzylamine, and *i*PrOH were present in larger quantities, and *N*-isopropylbenzylamine was present in trace amounts. Additionally, GC–MS analysis of the reaction solution was performed (Figure 8). Benzylamine (a) was clearly identified (the mass spectra obtained for each peak are not shown) as the main component, and dibenzylamine (b), *N*-benzylidenebenzylamine (c), *N*-isopropylbenzylamine (d), 2-propanol (e), and toluene (f) were identified as side components. Additionally, trace amounts of aniline (g) and polyaromatic condensation products of benzylamine (h) were detected. The main reaction occurring during the solvothermal treatment is thus a condensation reaction of the benzylamine solvent, mainly with an-

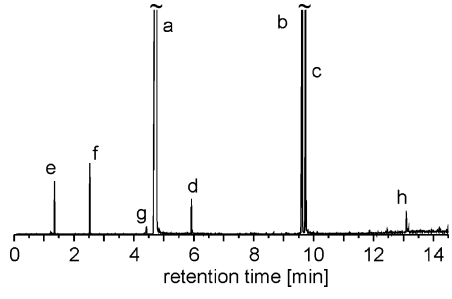

Figure 8. GC–MS spectrum of the reaction solution obtained after removal of the solid product from the benzylamine/$Ti(OiPr)_4$ system.

other solvent molecule, as illustrated in Scheme 1,A. It can be expected that the condensation is greatly catalyzed by the Ti centers present in the reaction system, as the high affinity of the amino groups to Ti alkoxides is well known from the studies of Cook in the 1950s.[26] As dibenzylamine forms, metal-coordinated ammonia groups remain, but these groups are not capable of inducing bridging to another metal center, as would be the case with hydroxy groups in the analogous ether elimination mechanism.[13,27] Instead of the nitride, the thermodynamically much more stable oxide is formed (see below), which implies that the ammonia groups must be released during the further course of the condensation. Indeed large quantities of ammonia were observed in the reaction system, which escaped upon opening the autoclave and were visible as a "boiling" of the reaction solution. The oxide formation hence must be induced by a different side reaction. For elucidation of this reaction, we compared the ratios of the main compounds detected by GC–MS, which were calculated to be benzylamine/*i*PrOH/toluene/dibenzylamine/*N*-benzylidenebenzylamine/*N*-isopropylbenzylamine, 99:1.0:1.9:17:15:1.1. It is remarkable that the ratio of detected isopropoxy groups to benzylamine is only half (100:2) of that used initially (100:4). As no remaining $Ti(OiPr)_4$ was detected in the system by NMR spectroscopic measurements, this indicates that half of the isopropoxy groups must have been converted into volatile compounds during the synthesis. Hence, we expect the elimination of the isopropoxy ligands of the titanium alkoxide to be the main mechanism for the formation of anatase, which leads to gaseous propene as a by-product (Scheme 1,B). This results in Ti–OH groups that then initiate the formation of oxygen bridges as the starting point of oxide formation [probably through release of 2-propanol from a second $Ti(OiPr)_4$ species]. Through further exchange reactions, *N*-isopropylbenzylamine is also formed. The vital point in this mechanism is the obviously high affinity of the amine nitrogen atom towards the metal alkoxide but, at the same time, its inability to form bridges between the metal centers. The same phenomenon has been observed similarly for the reaction of metal acetylacetonates in benzylamine,[28] and therefore, we postulate that the synthesis of metal nitrides in amine solvents cannot be achieved under standard sol–gel conditions from metal alkoxides.

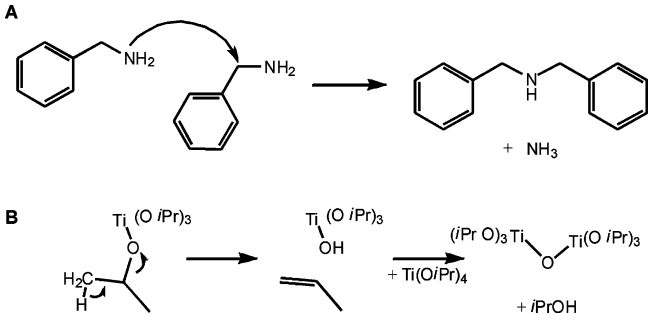

Scheme 1. Proposed reaction mechanisms occurring during the solvothermal treatment of $Ti(OiPr)_4$ in benzylamine.

Conclusions

A simple one-pot solvothermal reaction of titanium isopropoxide in benzylamine has been shown to result in remarkably complex, highly ordered nanostructures. These composites consist of anatase nanoplatelets that are assembled into larger sheet-like structures. The sheets are stacked in a highly ordered fashion, with thin organic layers in between them acting as "glue". We have shown that benzylamine is the only organic species found within this nanostructure, and therefore, we infer that the solvent plays many roles in the course of this synthesis. The solvent is already involved in the reaction mechanism leading to the transformation of the titanium isopropoxide into anatase. By selective capping of the (001) crystal face, benzylamine also controls the morphology of the forming crystals, by aggravating their growth in the [001] direction, which leads to the formation of nanoplatelets. The benzylamine species bound to the (001) surfaces next interact with each other, through π–π interactions, driving the stacking of the nanoplatelets into highly ordered lamellar superstructures. Similar solvents such as *m*-xylylenediamine are also capable of such multistage control, resulting in ordered structures with slightly larger spacing between the nanocrystals. These results show that aromatic amine solvents are highly interesting media for the formation of inorganic nanostructures by nonaqueous processes due to their versatile properties and their ability to selectively bind to specific faces of the forming nanocrystals.

Experimental Section

Synthesis: The solvents benzylamine and *m*-xylylenediamine were used as received in p.a./dry quality by Acros Organics and Aldrich. The samples were assembled in a glove box under an atmosphere of argon to exclude any influence of moisture and oxygen. The subsequent solvothermal treatment was performed in acid digestion bombs obtained by Parr Instruments, equipped with 45-mL Teflon cup holders. The appropriate amount of titanium tetraisopropoxide [$Ti(OiPr)_4$, 99.999%] was put into a 45-mL Teflon liner. Next, benzylamine or *m*-xylylenediamine (20 mL) was slowly added, and the Teflon liner was inserted into a steel autoclave, which was closed, removed from the glove box, and put into an oven that was preheated to 200 °C. After 3 d, the autoclave was removed from the oven and opened in air after cooling down. Caution must be taken when opening the autoclave due to possible overpressure of formed ammonia. In most cases, turbid suspensions resulted, from which the solid product was removed by centrifugation, and was washed by adding EtOH and CH_2Cl_2, followed by shaking and centrifugation. The powders were dried at room temperature in a desiccator.

Characterization: XRD measurements were carried out by using a Bruker D8 diffractometer equipped with a scintillation counter. The samples were measured in θ–θ reflection mode (under Cu-K_α radiation) by step-scanning with a step size of 0.04°. TEM was performed with a Zeiss EM 912Ω instrument at an acceleration voltage of 120 kV and a LEO 922 instrument at 200 kV. The samples were prepared by dispersing a small amount of powder in ethanol, followed by ultrasonication for 10 min and application of one drop of the dispersion on a carbon-coated copper grid (400 mesh).

DRIFTS measurements were carried out with a Bruker Equinox IFS 55 device under ambient atmosphere, under accumulation of 64 scans. TGA measurements were performed with a Mettler Toledo TGA/SDTA851 instrument under a nitrogen atmosphere by employing a heating rate of 5 °C min^{-1} from room temperature to 950 °C. The liquid-state ^{13}C NMR measurements were performed under ^{1}H-BB decoupling at 100 MHz, using $CDCl_3$ as solvent. The relevant main reaction products identified for the individual systems show the following shifts: (a) benzylamine/Ti(O*i*Pr)$_4$ system: dibenzylamine δ = 140.3 (Ph_{ipso}), other Ph signals superimposed by benzylamine, 53.1 (CH_2); *N*-benzylidenebenzylamine δ = 161.8 (C=N), 139.3/136.2 (Ph_{ipso}), 130.7 (Ph_{para}), 65.0 (CH_2); *N*-isopropylbenzylamine: δ = 136.5 (Ph_{ipso}), 51.6 (CH_2), 48.0 (CH), 22.9 (CH_3). Solid-state NMR analysis of the benzylamine nanocomposite was performed by using the CP-MAS $^{13}C\{^{1}H\}$ technique at 100 MHz. The sample was spun at 7 and 5 kHz. GC–MS analysis was carried out with a GC 6890N device by Agilent Technologies.

Acknowledgments

We thank Prof. L. Ernst and Dr. K. Ibrom, Central NMR Facilities, TU Braunschweig, for solid-state NMR measurements. R. Pitschke is acknowledged for the TEM measurements, and Prof. H. Menzel, Institute of Technical Chemistry, TU Braunschweig, is acknowledged for use of the DRIFTS instrument. N. T. thanks the Alexander von Humboldt Foundation for a research fellowship.

[1] Y. Chujo, *Curr. Opin. Solid State Mater. Sci.* **1996**, *1*, 806.
[2] P. Gomez-Romero, *Adv. Mater.* **2001**, *13*, 163.
[3] S. Komarneni, *J. Mater. Chem.* **1992**, *2*, 1219.
[4] U. Schubert, *Chem. Mater.* **2001**, *13*, 3487.
[5] G. Schmidt, M. M. Malwitz, *Curr. Opin. Colloid Interf. Sci.* **2003**, *8*, 103.
[6] U. Schubert, N. Hüsing, A. Lorenz, *Chem. Mater.* **1995**, *7*, 2010.
[7] J. Wen, G. L. Wilkes, *Chem. Mater.* **1996**, *8*, 1667.
[8] F. Ribot, C. Sanchez, *Comments Inorg. Chem.* **1999**, *20*, 327.
[9] Y.-W. Jun, J.-S. Choi, J. Cheon, *Angew. Chem.* **2006**, *118*, 3492; *Angew. Chem. Int. Ed.* **2006**, *45*, 3414.
[10] J. Park, J. Joo, S. G. Kwon, Y. Jang, T. Hyeon, *Angew. Chem.* **2007**, *119*, 4714; *Angew. Chem. Int. Ed.* **2007**, *46*, 4630.
[11] J. Park, K. An, Y. Hwang, J.-G. Park, H.-J. Noh, J.-Y. Kim, J.-H. Park, N.-M. Hwang, T. Hyeon, *Nat. Mater.* **2004**, *3*, 891.
[12] G. Garnweitner, L. M. Goldenberg, O. V. Sakhno, M. Antonietti, M. Niederberger, J. Stumpe, *Small* **2007**, *3*, 1626.
[13] M. Niederberger, G. Garnweitner, *Chem. Eur. J.* **2006**, *12*, 7282.
[14] N. Pinna, G. Garnweitner, P. Beato, M. Niederberger, M. Antonietti, *Small* **2005**, *1*, 113.
[15] M. Karmaoui, R. A. Sá Ferreira, A. T. Mane, L. D. Carlos, N. Pinna, *Chem. Mater.* **2006**, *18*, 4493.
[16] M. Karmaoui, L. Mafra, R. A. Sá Ferreira, J. Rocha, L. D. Carlos, N. Pinna, *J. Phys. Chem. C* **2007**, *111*, 2539.
[17] M. Niederberger, G. Garnweitner, J. Buha, J. Polleux, J. Ba, N. Pinna, *J. Sol-Gel Sci. Technol.* **2006**, *40*, 259.
[18] M. Niederberger, M. H. Bartl, G. D. Stucky, *J. Am. Chem. Soc.* **2002**, *124*, 13642.
[19] M. Niederberger, M. H. Bartl, G. D. Stucky, *Chem. Mater.* **2002**, *14*, 4364.
[20] G. Garnweitner, M. Antonietti, M. Niederberger, *Chem. Commun.* **2005**, 397.
[21] J. Polleux, N. Pinna, M. Antonietti, C. Hess, U. Wild, R. Schlögl, M. Niederberger, *Chem. Eur. J.* **2005**, *11*, 3541.
[22] Z. Zhang, X. Zhong, S. Liu, D. Li, M. Han, *Angew. Chem.* **2005**, *117*, 2532; *Angew. Chem. Int. Ed.* **2005**, *44*, 3466.
[23] Y.-W. Jun, J.-H. Lee, J.-S. Choi, J. Cheon, *J. Phys. Chem. B* **2005**, *109*, 14795.
[24] S. Asokan, K. M. Krueger, V. L. Colvin, M. S. Wong, *Small* **2007**, *3*, 1164.
[25] Integrated Spectral Data Base System for Organic Compounds: http://www.aist.go.jp/RIODB/SDBS/.
[26] C. M. Cook, *J. Am. Chem. Soc.* **1959**, *81*, 3828.
[27] N. Pinna, G. Garnweitner, M. Antonietti, M. Niederberger, *Adv. Mater.* **2004**, *16*, 2196.
[28] N. Pinna, G. Garnweitner, M. Antonietti, M. Niederberger, *J. Am. Chem. Soc.* **2005**, *127*, 5608.

Received: September 16, 2007
Published Online: January 17, 2008

